Manufacturing Letters 36 (2023) 80–85

Contents lists available at ScienceDirect

Manufacturing Letters

journal homepage: www.elsevier.com/locate/mfglet

Letters

Vibration chiseling: A backward-moving cutting for the high-efficiency fabrication of short metallic microfibers

Zhiwei Li [a,b], Jianfu Zhang [a,b], Zhongpeng Zheng [a,b], Pingfa Feng [a,b,c], Dingwen Yu [a,b], Jianjian Wang [a,b,*]

[a] State Key Laboratory of Tribology in Advanced Equipment, Department of Mechanical Engineering, Tsinghua University, Beijing 100084, China
[b] Beijing Key Laboratory of Precision/Ultra-precision Manufacturing Equipments and Control, Department of Mechanical Engineering, Tsinghua University, Beijing 100084, China
[c] Division of Advanced Manufacturing, Tsinghua Shenzhen International Graduate School, Tsinghua University, Shenzhen 518029, China

ARTICLE INFO

Article history:
Received 12 February 2023
Received in revised form 19 March 2023
Accepted 17 April 2023
Available online 4 May 2023

Keywords:
Metallic short fiber
Parallelogram-shaped vibration
Backward-moving cutting

ABSTRACT

This study proposes a rapid process for fabricating metallic microfibers: vibration chiseling. A parallelogram-shaped vibration is superimposed on the tool using a two-dimensional non-resonant vibration device, while the tool moves backward relative to conventional cutting. In this way, the material can be chiseled out from the surface as a chip during each vibration cycle to form a microfiber. Increasing the tool vibration frequency allows the short fibers to be produced rapidly. The tool vibration trajectory, tool shape, backward-moving velocity, and depth of cut (DoC) are the crucial parameters that control the microfiber's geometries. Machining tests have been conducted on copper under different tool-moving velocities and DoC to verify the efficacy of the proposed process. Copper microfibers with a length of tens to hundreds of microns and a diameter of $2 \sim 4$ μm have been successfully fabricated, demonstrating that vibration chiseling has good reproducibility, controllability, and efficiency.

© 2023 Society of Manufacturing Engineers (SME). Published by Elsevier Ltd. All rights reserved.

1. Introduction

Metallic microfibers are increasingly used in industrial applications due to their excellent thermal corrosion resistance, thermal conductivity, and electric conductivity [1–3]. They exist in different forms and diameters, including long, continuous, and short fibers [4]. In particular, short microfiber is defined as fiber with a length/diameter ratio of less than 100 [5], which has been widely applied in composites, filtration, biomedicine, et al. For example, the metal matrix composite reinforced by short metallic microfibers provides higher structural strength, stiffness, and fatigue life [4,6,7]. The sintered filtration fabricated by short metallic microfibers in combination with metal powders has a high level of filtration with unique permeability [8–10]. In addition, short metallic microfibers can be used in biomedical testing to facilitate disease detection [11]. The application progress of metallic short microfibers relies on high-throughput and cost-effective fabrication.

Currently, the fabrication methods for metallic microfibers mainly include bundle drawing [12], melt spinning [13], and cutting [5]. Bundle drawing is the most widely used manufacturing process for metallic fibers due to its high efficiency [4]. Thousands of wires tied together are stretched through a mold to generate fibers with the required diameter [14]. However, it is difficult for bundle drawing to process short microfibers due to the limitation of cutting fibers off. Melt spinning can produce continuous fibers via the rapid solidification of liquid metal using a rotating cooled wheel. However, the fabricated fibers by melt spinning are frequently coarse, and the fiber's diameter cannot be down to 10 μm [15]. Cutting using multi-tooth tool cuts metal fibers from the workpiece clamped on the machine tool [16,17], which is more suitable for fabricating long, continuous metallic microfibers than short metallic microfibers. The other cutting process, nanoskiving, could also be used to process short metallic microfibers with a width of less than one μm [18,19]. However, nanoskiving has the drawbacks of low efficiency and tedious procedure. So, it is still a challenging problem to fabricate short metallic microfibers rapidly and in large quantities.

This study proposes a vibration chiseling process to fabricate short metallic microfibers rapidly. In vibration chiseling, a parallelogram-shaped vibration trajectory is added to the tool, which moves in the backward direction. As a result, vibration chiseling can fabricate short metallic microfibers with a uniform shape and controllable length, which makes up for the shortcomings of existing methods.

* Corresponding author at: State Key Laboratory of Tribology in Advanced Equipment, Department of Mechanical Engineering, Tsinghua University, Beijing 100084, China.
E-mail address: wangjjthu@mail.tsinghua.edu.cn (J. Wang).

https://doi.org/10.1016/j.mfglet.2023.04.002
2213-8463/© 2023 Society of Manufacturing Engineers (SME). Published by Elsevier Ltd. All rights reserved.

2. Process principle of vibration chiseling

The principle of vibration chiseling is illustrated in Fig. 1. A parallelogram-shaped vibration is superimposed on the diamond tool, which simultaneously moves in the backward direction relative to conventional cutting. The parallelogram-shaped tool vibration coupling with its backward motion forms a unique overlapping tool trajectory, enabling the tool to chisel the material from the surface in each vibration cycle to produce a short microfiber. The chiseling process in one vibration cycle can be separated into four steps, as shown in Fig. 1**b**. First, the tool moves backward from the start point along the workpiece surface. Then, the tool chisels into the workpiece surface along the DoC direction to cut apart the material. Third, the tool moves forward to cut off the material to generate a microfiber. Finally, the tool moves upward to the workpiece surface to start a new cutting cycle. Since each vibration cycle produces one microfiber, the chiseling can be very efficient by adopting a high vibration frequency.

The crucial processing parameters of vibration chiseling controlling microfibers' geometries are the tool vibration (trajectory and frequency f), nominal moving velocity V_c, tool shape, and DoC. For example, as shown in Fig. 1**b**, the length of microfiber is governed by the tool nose radius and DoC. The width of microfiber can be controlled by the DoC and vibration trajectory. And the thickness of microfiber is determined by V_c/f and the vibration trajectory. Since these processing parameters are easily kept constant, the shape of fabricated microfibers can be highly uniform, giving vibration chiseling high process controllability and reproducibility.

3. Experimental design

A series of machining experiments were carried out to verify the efficacy of the proposed vibration chiseling. The experiment platform consists of a three-axis stage (Aerotech, ANT 130) and a linear actuator (Aerotech, ACT 165), as shown in Fig. 2**a**. A copper workpiece is fixed on the three-axis stage through an inclination stage, which is for level adjustment with the help of a capacitive displacement sensor (MicroSense probe 5810). The three-axis stage can provide the control of DoC. In addition, a 2D non-resonant vibration device is mounted on the linear actuator to provide the tool's moving motion relative to the workpiece. A single-point circular diamond tool (Yuhe, nose radius: 3 mm, rake angle: 0°, clearance: 10°) is fixed on the end effector of the vibration device.

The 2D vibration device is used to generate the parallelogram-shaped tool vibration. The vibration device's mechanical design and control scheme is illustrated in Fig. 2b. The device uses two piezoelectric stacks (Thorlabs PK4FQP1) to provide two vibrations in orthogonal directions. In addition, it adopts spring flexure hinges for vibration decoupling. The control signal is generated by an NI DAQ board (NI PCIE 6361), then amplified by a power amplifier (Piezodrive PX 200). As a result, the displacement-voltage control equation can be expressed:

$$\begin{bmatrix} X \\ Y \end{bmatrix} = \begin{bmatrix} A_{xL} & -A_{xR} \\ A_{yL} & A_{yR} \end{bmatrix} \begin{bmatrix} U_L \\ U_R \end{bmatrix}$$

Where X,Y are the displacements along the X, Y-axis, U_L and U_R are the input voltage of the left and right stacks, the coefficients

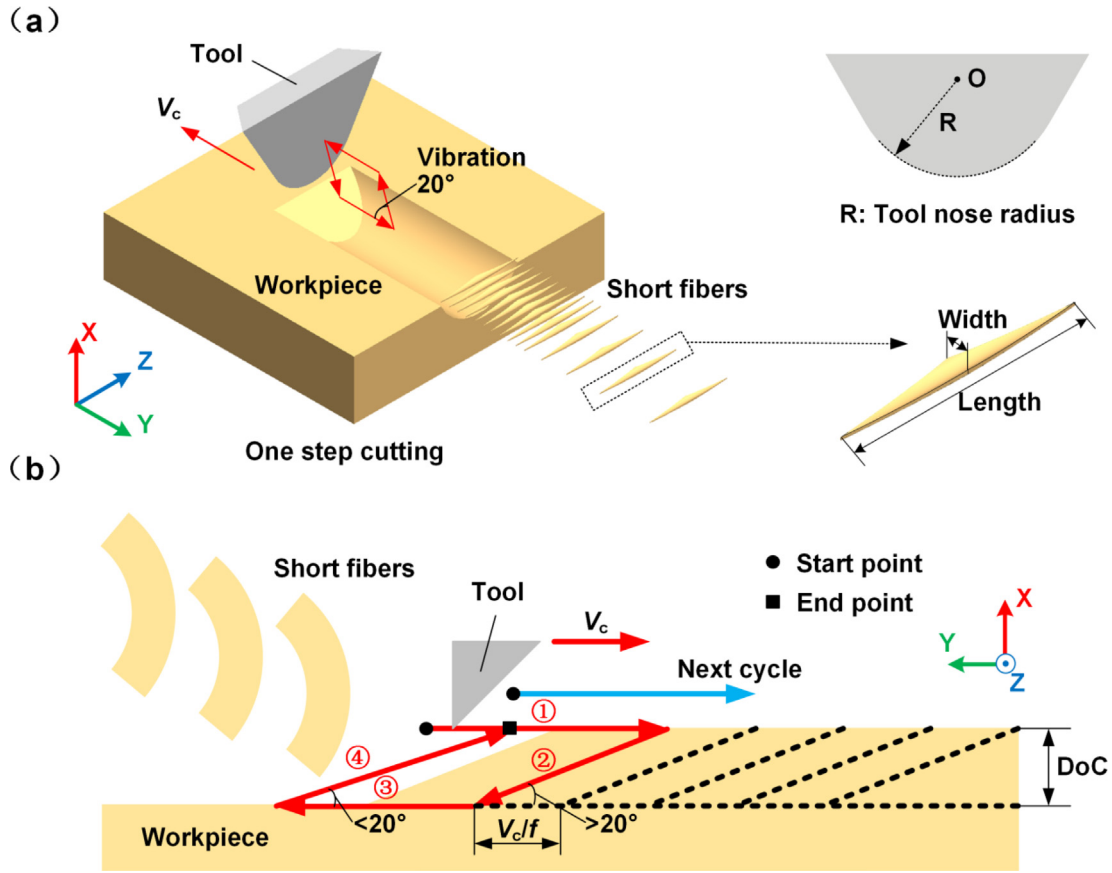

Fig. 1. Process principle of vibration chiseling. (a) 3D schematic diagram of vibration chiseling; (b) detained 2D schematic diagram of vibration chiseling.

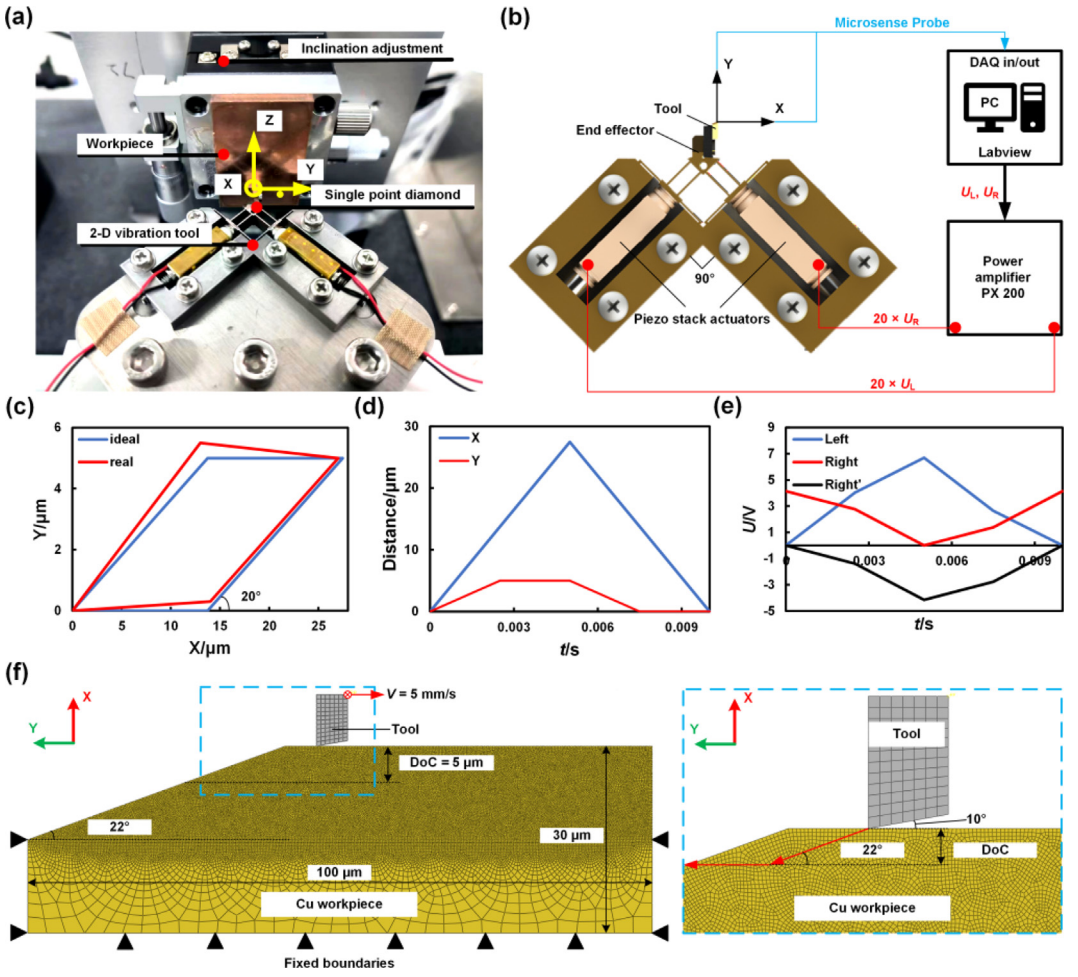

Fig. 2. Experimental and FEA setups. (a) Experimental setup; (b) 2D vibration device; (c) ideal and measured vibration trajectories; (d) displacement decomposition in X, Y directions; (e) input voltages of left and right piezoelectric stack; (f) FEA model.

A_{xL}, A_{xR}, A_{yL}, and A_{yR} have been obtained through vibration tests: A_{xL} = 1.26 μm/V, A_{xR} = 1.28 μm/V, A_{yL} = 0.92 μm/V, and A_{yR} = 0.88 μm/V. Using the control equation, the parallelogram-shaped tool vibration with a frequency of 100 Hz has been generated, with measurement results shown in Fig. 2**c**. The length and height of the parallelogram are 13.7 and 5 μm, respectively. The tool displacements and input voltages in two directions are shown in Fig. 2**d and e**.

The machining experiments consist of tool forward-moving and backward-moving cutting for comparison. The experiments are performed under different DoC (0 ∼ 5 μm) and tool moving velocities (0.1 ∼ 1 mm/s). The machining process was photographed in situ using a digital microscope (Leipan MS5, 100X). After the machining experiment, a scanning electron microscope (ZEISS, sigma 500) was used to observe the copper surface and analyze the geometries of the obtained microfibers.

Moreover, to further explore the fiber generation mechanism in vibration chiseling, a finite element analysis (FEA) model was developed using Abaqus 6.14. The geometric model (100 × 30 μm) and boundary conditions of the FEA are shown in Fig. 2**f**. The backward-moving velocity is set as 5 mm/s, and the DoC is 5 μm. The mechanical properties and the Johnson-Cook constitutive parameters used in the FEA are shown in Table 1 [20–22].

4. Results and discussion

Copper short microfibers with uniform shapes have been successfully fabricated using the proposed vibration chiseling process. The experimental results for forward- and backward-moving cutting under the same tool vibration trajectories are compared in Fig. 3 (See the attached videos 1 and 2 for details of the machining process). Separated microfibers regularly lie on the copper workpiece surface in vibration chiseling using the backward-moving tool. The microfibers have a fine curved spindle shape due to the circular arc of the tool nose. The length of the microfiber is 323 μm, the width is 4 μm, and the sharp angles of the two ends are 15.6° and 16°, respectively. In contrast, only a continuous chip appears on the copper workpiece surface in the tool's forward-moving vibration cutting. These results demonstrate that the backward tool moving is requisite for the vibration chiseling process.

In addition to the backward tool moving, the parallelogram-shaped tool vibration also plays a critical role in the vibration chiseling. The FEA results demonstrate the impact of the tool vibration: structural separation, shape control, and fiber forming, as shown **in** Fig. 4**a**. In one vibration cycle, the tool first cuts into the cupper surface and gradually cuts apart the material along the parallelogram's right hypotenuse; then the fiber forms in the process with a visible stress concentration; the tool moves back in the horizontal direction and completely separates the fiber from the workpiece. The simulated results of fiber generation correspond well with the experimental results that the produced short microfibers have a curved spindle shape. Besides, an apparent stress concentration occurs on the interface between the tool flank face and material. This stress concentration is because the tool clearance angle (10°) is smaller than the cutting path's inclination angle (22°), which induces the interaction of the tool flank face with

Table 1
Mechanical properties and Johnson-Cook constitutive parameters of copper.

Density (kg/m^3)	Elastic modulus (GPa)	Poisson's Ratio	Thermal conductivity (W/m·K)	Specific heat (J/kg·K)
8940	100	0.31	386	383
***A*/MPa**	***B*/MPa**	***n***	***C***	***m***
99.7	263	0.23	0.029	0.98

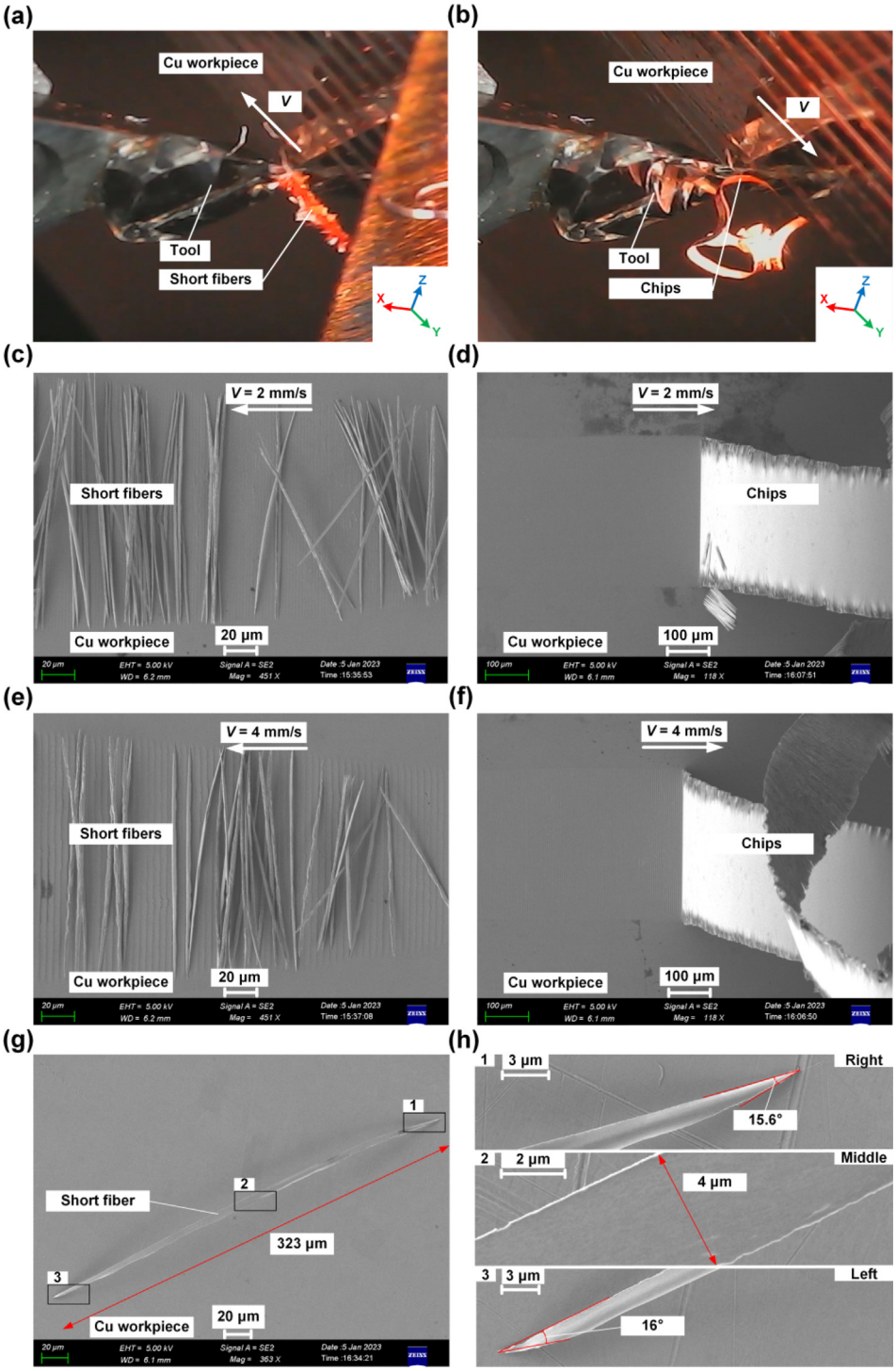

Fig. 3. Machining results comparison between tool forward- and backward-moving cutting. (a)(c)(e)(g)(h): backward-moving cutting; (b)(d)(f): forward-moving cutting.

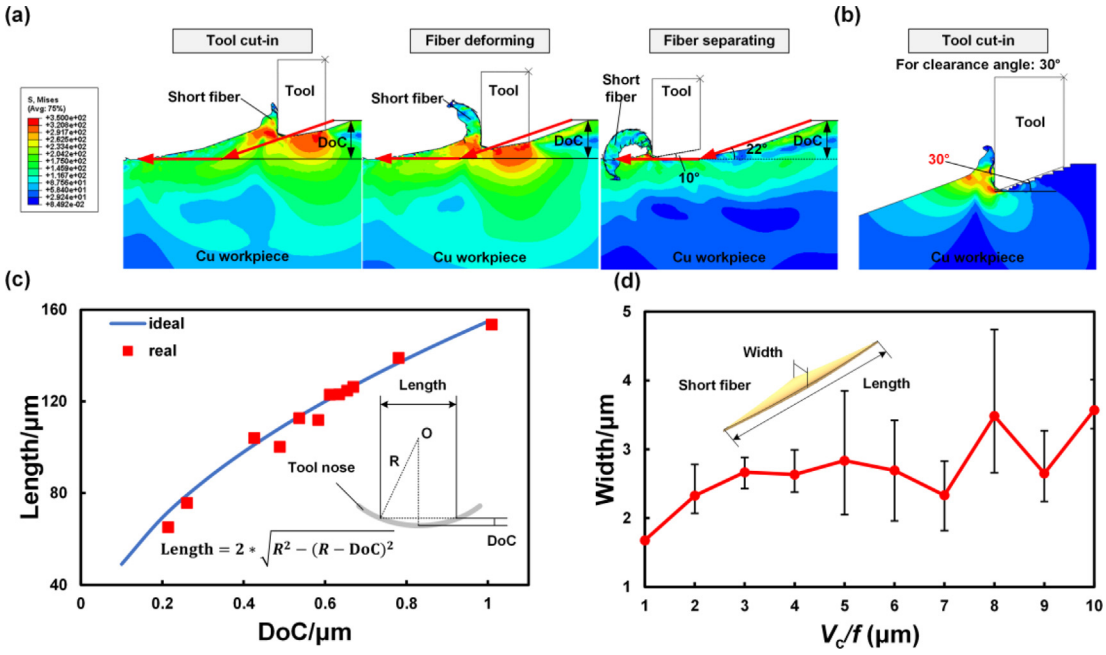

Fig. 4. FEA simulation and shape of microfibers. (a) FEA of fiber generation; (b) FEA for the tool clearance angle of 30°; (c) length of microfiber; (d) width of microfiber. The number of samples is five.

the workpiece material. As copper is a typical easy-to-cut material, this stress concentration would not cause extensive tool wear, which was not found in the experiment. However, progressive tool wear may be stimulated by this stress concentration. FEA with a larger tool clearance angle of 30° has been performed with results shown in Fig. 4b (the color bar is the same for all FEA). No significant interaction of the tool flank face with the workpiece material can be identified. Therefore, the tool flank face and material interaction can be avoided by the tool design with a larger clearance angle (the clearance angle needs to be larger than the cutting path's inclination angle).

The vibration chiseling demonstrates excellent process controllability regarding the shape of microfibers. Fig. 4**c** shows the measurement results of the length of fabricated microfibers, as well as the theoretical dependency of the length of microfibers on the DoC and tool nose radius. The experimental results show that the length of microfibers increases with the DoC, which agrees well with the theoretical results. Fig. 4**d** shows the statistical results of the width under different V_c/f. Overall, with the increase of the period V_c/f, the width gradually tends to increase. However, the width interval is mainly between 2 and 4 μm due to the limitations of the selected processing parameters. Copper nanowires with a width of less than 1 μm could be fabricated using the vibration chiseling process with reduced V_c/f. Moreover, the vibration chiseling is not limited to copper material. Metallic materials with excellent plasticity and machinability, such as gold, silver, and aluminum, can be processed by vibration chiseling to fabricate microfibers. Besides, the processing efficiency could be increased hundreds of times using an ultrasonic vibration device to substitute the parallelogram with a slim ellipse.

The collecting, handling, and stacking are necessary procedures before applying microfibers. During processing, the generated short metallic microfibers are overlaid on the surface and easy to collect, as shown in the attached video 1. Then, the collected microfibers are cleaned using an ultrasonic cleaner with agents like anhydrous ethanol and dried in the air. After the procedures above, the microfibers can be packed into a drying box for further use. However, the fabricated microfibers are challenging to stack due to their length and cross-section, though it is unnecessary to stack them regularly for some applications such as filtration and composites.

The microfibers generated by vibration chiseling have curved cross-section that strongly differs from the shape of the fibers generated by the established alternatives like bundle drawing. This unique curved cross-section would be beneficial or harmful for different applications. For example, curved structures can form more holes to improve the filterability of the filter. They can also provide more reaction sites for the high-performance microreactor. However, for the application of metallic fiber composites, the strength of microfiber with a curved cross-section may not be large enough.

5. Conclusion

This study proposes a vibration chiseling process for rapidly fabricating metallic microfibers. A 2D non-resonant vibration cutting device is used to generate a parallelogram-shaped tool vibration trajectory. Machining tests and FEA are conducted to verify the efficacy and explore the underlying process mechanism of vibration chiseling. The main conclusions can be drawn as follows:

(1) In vibration chiseling, the parallelogram-shaped tool vibration coupling with its backward motion forms a unique overlapping tool trajectory, which makes the material chiseled out in each vibration cycle to produce a short microfiber. Uniform copper short microfibers with a curved spindle shape (a length of tens to hundreds of microns) have been successfully fabricated, verifying the efficacy of vibration chiseling.
(2) Backward tool moving and parallelogram-shaped vibration are requisites for vibration chiseling. A continuous chip rather than separated fiber is generated if the tool moves in the conventional forward direction. FEA demonstrates that the parallelogram-shaped vibration divides the chiseling process into tool cut-in, chip deforming, and fiber separating in each vibration cycle.
(3) Vibration chiseling has the advantage of high efficiency, reproducibility, and shape controllability, especially for the length of metallic microfibers. Tool vibration (trajectory

and frequency f), nominal moving velocity V_c, tool shape, and DoC are the crucial processing parameters that control microfibers' geometries. The length of microfiber has a positive correlation with DoC and too nose radius. The width of microfiber gradually increases with the increase of the period V_c/f.

Declaration of Competing Interest

The authors declare that they have no known competing financial interests or personal relationships that could have appeared to influence the work reported in this paper.

Acknowledgments

The authors gratefully acknowledge the financial support for this research provided by the National Natural Science Foundation of China (Grant No. 52105458); Beijing Natural Science Foundation [Grant No. 3222009]; Tsinghua-Foshan Innovation Special Fund [No:2021THFS0204]; Huaneng Group Science and Technology Research Project (No: HNKJ22-U22YYJC08).

Appendix A. Supplementary data

Supplementary data to this article can be found online at https://doi.org/10.1016/j.mfglet.2023.04.002.

References

[1] Sun J, Xu S, Lu G, Ruan D, Wang Q. Mechanical response of fibre metal laminates (FMLs) under low to intermediate strain rate tension. Compos Struct 2023;305:116493.
[2] Dai X, Yang F, Yang R, Lee YC, Li C. Micromembrane-enhanced capillary evaporation. Int J Heat Mass Transf 2013;64:1101–8.
[3] Gong S, Schwalb W, Wang Y, Chen Y, Tang Y, Si J, et al. A wearable and highly sensitive pressure sensor with ultrathin gold nanowires. Nat Commun 2014;5:3132.
[4] Akhil MG, Arsha AG, Manoj V, Rajan TPD, Pai BC, Huber P, et al. 17 - Metal fiber reinforced composites. In: Joseph K, Oksman K, George G, Wilson R, Appukuttan S, editors. Fiber Reinforced Composites. Woodhead Publishing; 2021. p. 479–513.
[5] Veit D. in: Fibers: History, Production, Properties, Market, Springer International Publishing, Cham, 2022, pp. 941-956.
[6] Tevatia A, Srivastava SK. Modified shear lag theory based fatigue crack growth life prediction model for short-fiber reinforced metal matrix composites. Int J Fatigue 2015;70:123–9.
[7] Kurumlu D, Payton EJ, Somsen C, Dlouhy A, Eggeler G. On the presence of work-hardened zones around fibers in a short-fiber-reinforced Al metal matrix composite. Acta Mater 2012;60:6051–64.
[8] Kamp C, Folino P, Wang Y, Sappok A, Ernstmeyer J, Saeid A, et al. Ash Accumulation and Impact on Sintered Metal Fiber Diesel Particulate Filters. SAE Int J Fuels Lubr 2015;8.
[9] Huang X, Wang Q, Zhou W, Deng D, Zhao Y, Wen D, et al. Morphology and transport properties of fibrous porous media. Powder Technol 2015;283:618–26.
[10] Seok J, Chun KM, Song S, Lee S. Study on the filtration behavior of a metal fiber filter as a function of filter pore size and fiber diameter. J Aerosol Sci 2015;81:47–61.
[11] Yoo SM, Kang M, Kang T, Kim DM, Lee SY, Kim B. Electrotriggered, spatioselective, quantitative gene delivery into a single cell nucleus by Au nanowire nanoinjector. Nano Lett 2013;13:2431–5.
[12] Celentano DJ, Palacios MA, Rojas EL, Cruchaga MA, Artigas AA, Monsalve AE. Simulation and experimental validation of multiple-step wire drawing processes. Finite Elem Anal Des 2009;45:163–80.
[13] Kirstein T. 1 - The future of smart-textiles development: new enabling technologies, commercialization and market trends. In: Kirstein T, editor. Multidisciplinary Know-How for Smart-Textiles Developers. Woodhead Publishing; 2013. p. 1–25.
[14] Yang K, Guan SJ, Wang XD. The Design & Calculation for Hydraulic Cylinder of a Special Machine for Heat Exchanger Tube Bundle Drawing and Assembling. Appl Mech Mater 2014;496–500:789–92.
[15] Albracht F. Metallfasern als schallabsorbierende Strukturen und als leitfähige Komponenten in Verbundwerkstoffen, (2004).
[16] Yuan W, Tang Y, Yang X, Liu B, Wan Z. On the processing and morphological aspects of metal fibers based on low-speed multi-tooth dry cutting. Int J Adv Manuf Technol 2012;66:1147–57.
[17] Zhou W, Li S, Liu R, Chu X. Experimental and simulation investigation of multi-tooth cutting process of long fiber using copper wire continuous feeding. J Mater Process Technol 2019;273.
[18] Dong Z, Yan Y, Peng G, Li C, Geng Y. Effects of sandwiched film thickness and cutting tool water contact angle on the processing outcomes in nanoskiving of nanowires. Mater Des 2023;225:111438.
[19] Fang Z, Yan Y, Geng Y. Uncovering the machining mechanism of polycrystalline gold nanowires by nanoskiving. Int J Mech Sci 2022;230:107545.
[20] Yin S, Wang X, Xu B, Li W. Examination on the Calculation Method for Modeling the Multi-Particle Impact Process in Cold Spraying. J Therm Spray Technol 2010;19:1032–41.
[21] Zheng Z, Ni C, Yang Y, Bai Y, Jin X. Numerical Analysis of Serrated Chip Formation Mechanism with Johnson-Cook Parameters in Micro-Cutting of Ti6Al4V. Metals (Basel) 2021;11:102.
[22] J.J. Grazka M, Identification of Johnson-Cook Equation Constants using Finite Element Method, Engineering Transactions 3 (2012) 215–223.